JACS
JOURNAL OF THE AMERICAN CHEMICAL SOCIETY

COMMUNICATION

pubs.acs.org/JACS

Multivalent Binding Motifs for the Noncovalent Functionalization of Graphene

Jason A. Mann, Joaquín Rodríguez-López, Héctor D. Abruña,* and William R. Dichtel*

Department of Chemistry and Chemical Biology, Cornell University, Baker Laboratory, Ithaca, New York 14853-1301, United States

Supporting Information

ABSTRACT: Single-layer graphene is a newly available conductive material ideally suited for forming well-defined interfaces with electroactive compounds. Aromatic moieties typically interact with the graphene surface to maximize van der Waals interactions, predisposing most compounds to lie flat on its basal plane. Here we describe a tripodal motif that binds multivalently to graphene through three pyrene moieties and projects easily varied functionality away from the surface. The thermodynamic and kinetic binding parameters of a tripod bearing a redox-active Co(II) *bis*-terpyridyl complex were investigated electrochemically. The complex binds strongly to graphene and forms monolayers with a molecular footprint of 2.3 nm^2 and a $\Delta G_{ads} = -38.8 \pm 0.2$ kJ mol^{-1}. Its monolayers are stable in fresh electrolyte for more than 12 h and desorb from graphene 1000 times more slowly than model compounds bearing a single aromatic binding group. Differences in the heterogeneous rate constants of electron transfer between the two compounds suggest that the tripod projects its redox couple away from the graphene surface.

Graphene's desirable electronic, optical, and mechanical properties have attracted considerable interest.[1] Advances in its growth via metal-catalyzed chemical vapor deposition (CVD),[2] the thermal decomposition of SiC,[3] and chemical reduction of graphene oxide (GO)[4] now provide convenient access to large-area samples, including films on flexible substrates.[5] As a result, graphene shows promise for inexpensive transparent electrodes,[6] transistors,[7] strain sensors,[8] ultrathin corrosion barriers,[9] and many other applications. Graphene's single-atom thickness and atomically precise structure also make it an attractive platform for molecular assembly and interfacing functional π-electron systems to bulk electrodes[10] as well as a unique imaging platform for confined chemical transformations.[11] Modular and broadly applicable methods for functionalizing graphene's basal plane offer a means to manipulate its structure and/or electronic properties and will impact many of the above applications. Covalent approaches disrupt the conjugation and, thus, the electronic structure of the graphene sheet and take place preferentially at carbon atoms near defects and grain boundaries.[12] Noncovalent functionalization strategies do not suffer from these drawbacks.

Noncovalent functionalization has often focused on dispersing chemically converted graphene (CCG) in various solvents following reduction of GO. Compounds designed for this purpose interact with CCG either at graphitic sites or residual carboxylate defects.[13] The basal planes of exfoliated, epitaxial, or CVD graphene samples have been functionalized less frequently. Alkane thiols assembled on exfoliated graphene were used to detect Hg^{2+} ions at ppm levels.[14] Polycyclic aromatic compounds assemble into stable, ordered structures on epitaxial graphene[15] and can shift its Fermi level[16] or serve as nucleation sites for atomic layer deposition.[17] Xu et al. used pyrene butyrate to exfoliate graphite and disperse the resulting graphene layers in H_2O.[18] However, the strength of the pyrene−graphene interaction has not been reported, and individual pyrene rings lack the ability to precisely control the distance and orientation of pendant functionality relative to the surface. Compounds capable of binding graphene with well-defined, multivalent interactions can provide robust monolayers that display active functionality away from the graphene surface, enabling these moieties to interact predictably with other species in solution.

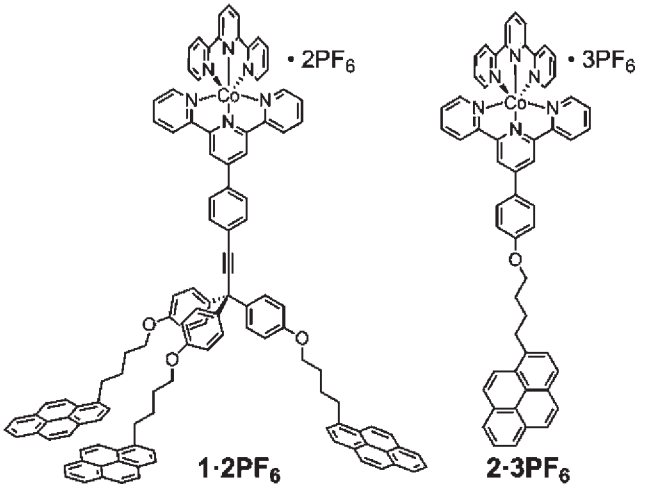

Figure 1. Structures of a tripodal graphene binder **1**·$2PF_6$ and monovalent model compound **2**·$3PF_6$, each bearing a redox-active Co(tpy) complex for electrochemical characterization of their binding properties.

Here we describe a tripodal binding motif (Figure 1), which presents three pyrene "feet" that interact with graphene substrates. Tripodal architectures have been used to functionalize Si,[19] Au,[20] and TiO_2[21] surfaces, where they have consistently demonstrated enhanced stability and orientational control relative to monovalent groups.[22] A Co(II) *bis*-terpyridyl complex ($[Co(tpy)_2]^{2+}$) was incorporated into the graphene-binding tripod **1**·$2PF_6$ to measure its binding constant and surface coverage

Received: August 31, 2011
Published: October 11, 2011

Scheme 1. Synthesis of Tripodal Graphene Binder 1·2PF6

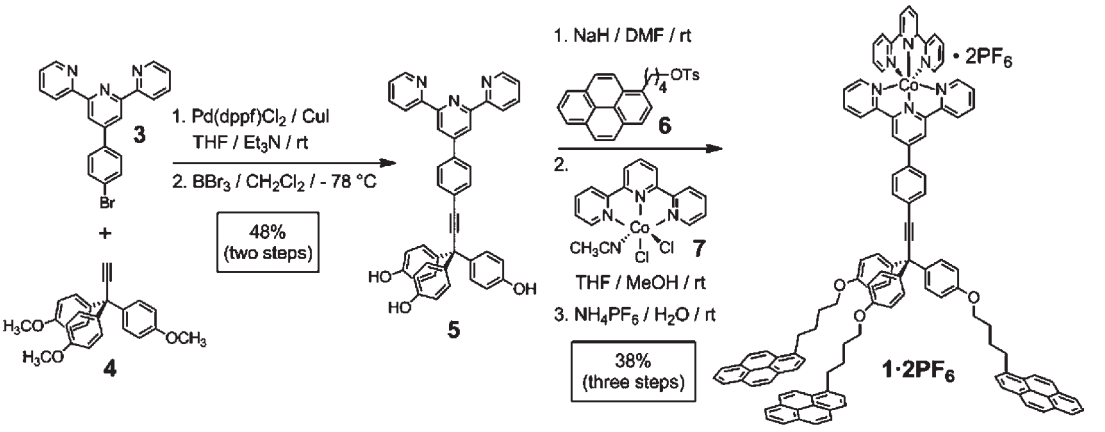

through electrochemical observation of the $Co^{2+/3+}$ redox couple. The characteristics of the monovalent $[Co(tpy)_2]^{3+}$ complex **2·3PF$_6$** were also determined electrochemically to elucidate the effect of multivalency on the coverage and stability of the monolayers. Working electrodes based on single-layer graphene were first reported only recently,[23] and the following experiments are the first to characterize molecular self-assembly on the graphene basal plane using electrochemistry.

The synthesis (Scheme 1) of the tripodal binding motif is modular, allowing future variation of both the aromatic binding groups and the presented functionality. Pyrene was selected as the binding group because it has been used extensively to functionalize carbon nanotubes.[24] The tetrahedral core **4** was established through the nucleophilic substitution of ethynyl magnesium bromide to tris(*p*-methoxyphenyl) methyl chloride. The terminal alkyne moiety of **4** was elaborated to a terpyridyl ligand through a Sonogashira cross-coupling, after which the three methoxy groups were demethylated with BBr_3. The resulting triphenol **5** was alkylated under Williamson etherification conditions by the pyrene tosylate **6**. The resulting tripodal ligand was metalated using excess $Co(tpy)Cl_2MeCN$ **7** to provide **1·2PF$_6$**. The Co^{2+} complex in **1·2PF$_6$** is paramagnetic, complicating assignment of its NMR resonances. Nevertheless, its spectrum was consistent with the presence of a single Co^{2+} species. Electrospray ionization (ESI) and matrix assisted laser desorption ionization (MALDI) mass spectrometry each indicated the formation of **1·2PF$_6$** and did not show peaks corresponding to other $Co(tpy)_2$ complexes. We also oxidized **1·2PF$_6$** to the corresponding diamagnetic Co^{3+} species using $AgPF_6$. The ^{1}H NMR spectrum of this complex indicated its structure and purity. We also synthesized the monopodal compound of similar structure **2·2PF$_6$**, though thin layer chromatography and ^{1}H NMR spectroscopy indicated that its terpyridyl ligands were substitutionally labile. $[Co(tpy)_2]^{+3}$ species are less prone to ligand exchange, and so we also oxidized **2·2PF$_6$** to the Co^{3+} species **2·3PF$_6$**, again using $AgPF_6$, to facilitate its characterization and storage.

Monolayer formation of the two compounds was characterized by cyclic voltammetry (CV) using a working electrode composed of CVD graphene transferred onto a silicon wafer (0.07 cm^2 active area, see Supporting Information (SI) for fabrication details). Pt counter and pseudoreference electrodes were used with analyte **1·2PF$_6$** or **2·3PF$_6$** in THF/NH_4PF_6 (0.1 M) supporting electrolyte. These experiments confirm adsorption of both complexes to the electrode surface. They also show chemically reversible but electrochemically quasi-reversible charge transfer kinetics for the $Co^{2+/3+}$ couple (*ca.* −0.2 V vs Fc/Fc^+), as indicated by their voltammetric wave-shape and changes in oxidative and reductive peak potentials (ΔE_p) as a function of sweep rate (Figure 2A). The linear dependences of the anodic and cathodic peak currents (see SI) on the potential sweep rate indicate that the redox couple is confined to the electrode surface.[25]

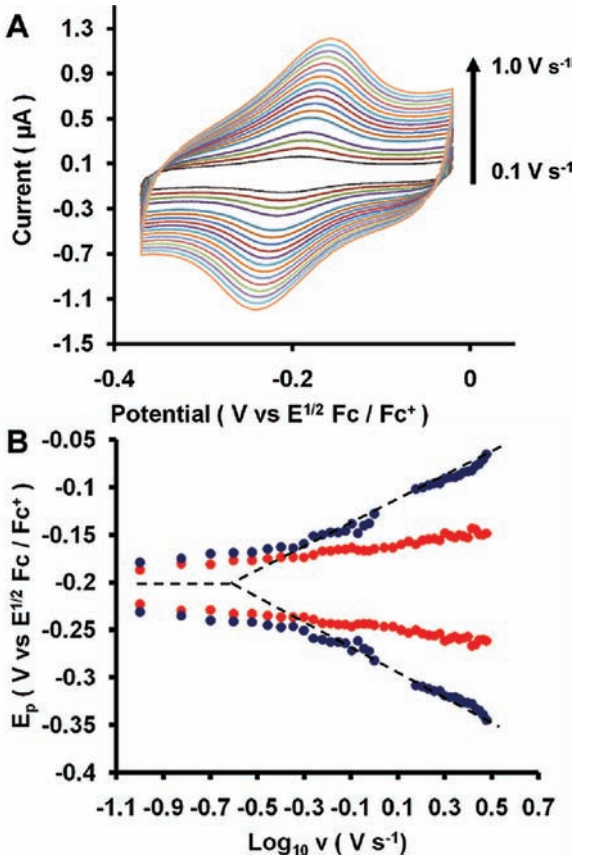

Figure 2. (A) Cyclic voltammograms of **1·2PF$_6$** (1 μM) obtained at various scan rates on an SLG working electrode in THF/NH_4PF_6 (0.1 M). (B) Laviron plots of **1·2PF$_6$** (blue) and **2·3PF$_6$** (red); peak potentials at different scan rates (0.1 V s^{-1} to 3.0 V s^{-1}) on SLG.

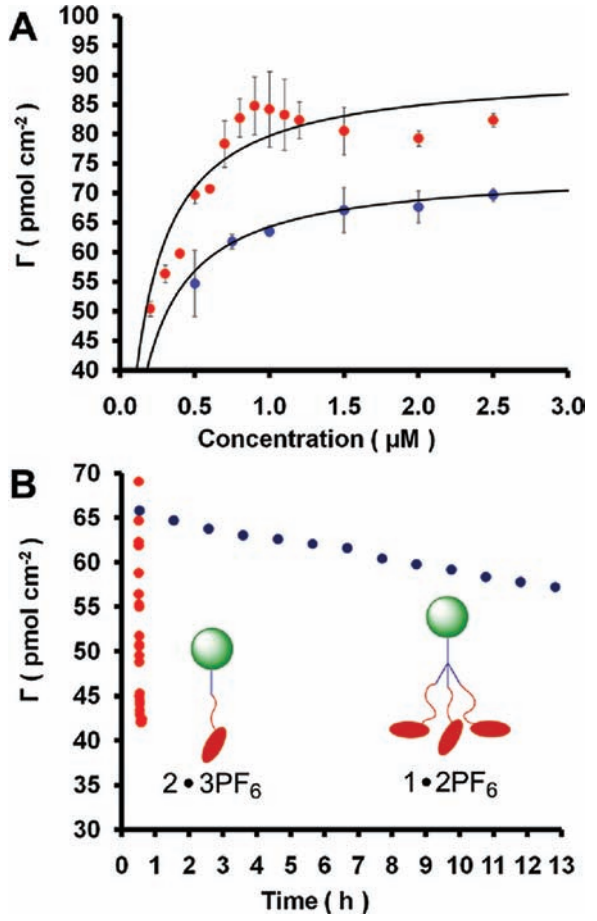

Figure 3. (A) Langmuir binding isotherms of $\mathbf{1\cdot 2PF_6}$ (blue) and $\mathbf{2\cdot 3PF_6}$ (red) on SLG derived from surface coverages measured at various concentrations (0.1−3 μM). (B) Plots of coverage (Γ) vs time for monolayers of $\mathbf{1\cdot 2PF_6}$ (blue) and $\mathbf{2\cdot 3PF_6}$ (red) monolayers that were formed on SLG electrodes, and then transferred to fresh THF/NH_4PF_6 (0.1 M) electrolyte solution at $t = 0$.

$\mathbf{1\cdot 2PF_6}$ was designed to project its $Co(tpy)_2$ redox probe away from the SLG surface, a degree of orientational control not found in monovalent binding groups. We performed Laviron analyses (Figure 2B) of the surface voltammetry[26] of both $\mathbf{1\cdot 2PF_6}$ and $\mathbf{2\cdot 3PF_6}$ to probe differences in electron transfer rates for the two binding motifs. For $\mathbf{1\cdot 2PF_6}$, the peak potentials (E_p) of the anodic and cathodic scans converge to the value of the formal potential $E^{o\prime}$ at low scan rates (ν), whereas larger peak separations are observed at higher scan rates. The symmetry and similar slope observed in the linear part of this plot for the anodic and cathodic branches suggest a transfer coefficient $\alpha \approx 0.5$, and analysis of the scan rate dependence (see SI) yields a heterogeneous charge transfer rate constant $k^\circ = 13.5\ s^{-1}$. Additionally, analysis of the shape of the CVs (see SI) suggests no lateral interactions between the $Co^{2+/3+}$ redox centers, such that monolayer formation may be described by the Langmuir model (see below). The Laviron plot for $\mathbf{2\cdot 3PF_6}$ shows smaller peak separations than $\mathbf{1\cdot 2PF_6}$ at equivalent scan rates, which indicates faster electron transfer kinetics with a rate constant $k^\circ \approx 18\ s^{-1}$ (see SI). The slower rate of electron transfer observed for $\mathbf{1\cdot 2PF_6}$ is consistent with the hypothesis that the tripod positions the redox center further away from the electrode than the monovalent model compound. Atomic force microscopy of the graphene electrodes before and after functionalization with the tripod showed no evidence for aggregation on the surface (see SI).

We integrated the peak currents in the CVs of $\mathbf{1\cdot 2PF_6}$ and $\mathbf{2\cdot 3PF_6}$ to obtain the total charge transferred (Q), from which the surface coverage (Γ) was calculated according to the relation $Q = nFA\Gamma$. Using the above method, we measured the surface coverage as a function of $[\mathbf{1\cdot 2PF_6}]$ or $[\mathbf{2\cdot 3PF_6}]$, respectively. These data were fit to the Langmuir isotherm model described by the equation $\Gamma = \Gamma_s Kc(Kc + 1)^{-1}$ (where K is the equilibrium constant of binding and c is the concentration of adsorbate in solution) to determine the thermodynamic binding parameters for the monopodal and tripodal motifs. The isotherm of $\mathbf{1\cdot 2PF_6}$ (Figure 3A) corresponds to a ΔG_{ads} of -38.8 ± 0.2 kJ mol^{-1} while the isotherm of $\mathbf{2\cdot 3PF_6}$ shows that it binds with a ΔG_{ads} of -38.3 ± 0.5 kJ mol^{-1}. Interestingly, the binding energies of the tripodal and monopodal compounds are similar, despite significant differences in the kinetic stability of the monolayers of the tripods (see below). It is possible that noncovalent interactions among the pyrene rings in the unbound form of $\mathbf{1\cdot 2PF_6}$ are disrupted upon binding to graphene, an energetic cost reflected in its ΔG_{ads}. We will revisit this consideration when designing future tripodal binding motifs.

The saturation coverage (Γ_s) of $\mathbf{1\cdot 2PF_6}$ is 73.9 ± 0.2 pmol cm^{-2}, which corresponds to a 2.3 nm^2 molecular footprint. The Γ_s of $\mathbf{2\cdot 3PF_6}$ is 90.7 ± 0.6 pmol cm^{-2}, a 1.7 nm^2 molecular footprint. The coverage of the monovalent binding compound is not significantly higher than that of the tripod, despite the tripod's larger size. This finding is consistent with our hypothesis that the $Co(tpy)_2$ complex of $\mathbf{2\cdot 3PF_6}$ weakly interacts with the graphene surface[27] and occupies a larger area on the surface than a single pyrene moiety. Thus, the tripodal design allows for improved orientational control of its functionality while maintaining comparable coverage.

Robust noncovalent functionalization requires that monolayers remain kinetically stable in the absence of excess adsorbate in solution. We evaluated the kinetic stability of monolayers of $\mathbf{1\cdot 2PF_6}$ and $\mathbf{2\cdot 3PF_6}$ by transferring functionalized graphene electrodes into blank electrolyte. The coverage of monovalent $\mathbf{2\cdot 3PF_6}$ rapidly diminished by 50% in just under 8 min, with a first-order rate constant $k = 1.4 \times 10^{-3}\ s^{-1}$ (Figure 3B). In contrast, $\mathbf{1\cdot 2PF_6}$ desorbed 1000 times more slowly, decreasing by only about 14% over 12 h, with a first-order rate constant $k = 3.5 \times 10^{-6}\ s^{-1}$ (Figure 3B). Thus, though compounds bearing a single pyrene bind to graphene, their monolayers rapidly desorb in organic solvents. Monolayers based on the tripodal binding motif are stable for hours under similar conditions, which should render them compatible with solution processing techniques, such as spin-coating or drop-casting, often employed during device fabrication. For example, we anticipate that appropriately functionalized tripod monolayers will serve as anchors for interfacing polymers or extended materials to the graphene surface, and that the kinetic stability of the tripod/graphene interaction will facilitate studies of molecular diffusion in two dimensions.

In conclusion, we have designed and synthesized a tripodal binding motif that adsorbs strongly on the basal plane of single-layer graphene. We also have measured, through electrochemistry, the kinetic and thermodynamic binding parameters of aromatic systems on graphene for the first time. The tripod projects variable functionality, here a $Co(tpy)_2$ redox probe, away from the graphene surface, as suggested by differences in rates of electron transfer between tripodal and monovalent binding units. Our kinetic experiments demonstrate that individual pyrene units readily desorb from graphene in organic solvents. In contrast, tripodal binding motifs form stable monolayers that withstand

infinite dilution conditions for hours. Future studies will focus on characterizing the structure and dynamics of this tripodal binding motif on the graphene surface using complementary spectroscopic and probe microscopy techniques. Graphene is both a new platform for molecular assembly and a technologically relevant electrode material, and specific noncovalent functionalization methods are needed to reliably control its interface to organic materials. Methods for preparing graphene with minimal defects and large grain size are advancing rapidly,[28] making functionalization of the pristine basal plane increasingly important. The orientational control and kinetic stability of monolayers of tripodal systems will enable their use as anchors in a wide variety of contexts, including for integrating molecular compounds, extended materials, and biomolecules for optoelectronic, catalysis, and biosensing applications.

■ ASSOCIATED CONTENT

Supporting Information. Experimental procedures, spectral data for all new compounds, additional electrochemical characterization, and complete ref 28b. This material is available free of charge via the Internet at http://pubs.acs.org.

■ AUTHOR INFORMATION

Corresponding Author
wdichtel@cornell.edu; hda1@cornell.edu

■ ACKNOWLEDGMENT

This research was supported by startup funds provided by Cornell University and the NSF-funded CCI-I Center for Molecular Interfacing (CHE-0847926). We also acknowledge NSF support through use of the Cornell Nanofabrication Facility/NNIN and the Cornell Center for Materials Research facilities. J.A.M. gratefully acknowledges the Integrative Graduate Education and Research Traineeship (IGERT) Program in the Nanoscale Control of Surfaces and Interfaces which is supported under NSF Award DGE-0654193, the Cornell Center for Materials Research, and Cornell University. We thank G. Gutierrez for preparation of intermediates, C. Tan for useful discussions, and S. Burkhardt for providing the TOC illustration.

■ REFERENCES

(1) (a) Allen, M. J.; Tung, V. C.; Kaner, R. B. *Chem. Rev.* **2009**, *110*, 132. (b) Geim, A. K. *Science* **2009**, *324*, 1530.

(2) (a) Levendorf, M. P.; Ruiz-Vargas, C. S.; Garg, S.; Park, J. *Nano Lett.* **2009**, *9*, 4479. (b) Li, X.; Cai, W.; An, J.; Kim, S.; Nah, J.; Yang, D.; Piner, R.; Velamakanni, A.; Jung, I.; Tutuc, E.; Banerjee, S. K.; Colombo, L.; Ruoff, R. S. *Science* **2009**, *324*, 1312. (c) Kim, K. S.; Zhao, Y.; Jang, H.; Lee, S. Y.; Kim, J. M.; Kim, K. S.; Ahn, J.-H.; Kim, P.; Choi, J.-Y.; Hong, B. H. *Nature* **2009**, *457*, 706. (d) Reina, A.; Jia, X.; Ho, J.; Nezich, D.; Son, H.; Bulovic, V.; Dresselhaus, M. S.; Kong, J. *Nano Lett.* **2008**, *9*, 30.

(3) Emtsev, K. V.; Bostwick, A.; Horn, K.; Jobst, J.; Kellogg, G. L.; Ley, L.; McChesney, J. L.; Ohta, T.; Reshanov, S. A.; Rohrl, J.; Rotenberg, E.; Schmid, A. K.; Waldmann, D.; Weber, H. B.; Seyller, T. *Nat. Mater.* **2009**, *8*, 203.

(4) (a) Zhu, Y.; Murali, S.; Cai, W.; Li, X.; Suk, J. W.; Potts, J. R.; Ruoff, R. S. *Adv. Mater.* **2010**, *22*, 3906. (b) Green, A. A.; Hersam, M. C. *J. Phys. Chem. Lett.* **2009**, *1*, 544.

(5) Choi, D.; Choi, M.-Y.; Choi, W. M.; Shin, H.-J.; Park, H.-K.; Seo, J.-S.; Park, J.; Yoon, S.-M.; Chae, S. J.; Lee, Y. H.; Kim, S.-W.; Choi, J.-Y.; Lee, S. Y.; Kim, J. M. *Adv. Mater.* **2010**, *22*, 2187.

(6) (a) Kumar, A.; Zhou, C. *ACS Nano* **2010**, *4*, 11. (b) Li, X.; Zhu, Y.; Cai, W.; Borysiak, M.; Han, B.; Chen, D.; Piner, R. D.; Colombo, L.; Ruoff, R. S. *Nano Lett.* **2009**, *9*, 4359.

(7) (a) Lee, W. H.; Park, J.; Sim, S. H.; Lim, S.; Kim, K. S.; Hong, B. H.; Cho, K. *J. Am. Chem. Soc.* **2011**, *133*, 4447. (b) Liu, W.; Jackson, B. L.; Zhu, J.; Miao, C.-Q.; Chung, C.-H.; Park, Y. J.; Sun, K.; Woo, J.; Xie, Y.-H. *ACS Nano* **2010**, *4*, 3927.

(8) Wang, Y.; Yang, R.; Shi, Z.; Zhang, L.; Shi, D.; Wang, E.; Zhang, G. *ACS Nano* 2011, ASAP DOI: 10.1021/nn103523t.

(9) Chen, S.; Brown, L.; Levendorf, M.; Cai, W.; Ju, S.-Y.; Edgeworth, J.; Li, X.; Magnuson, C. W.; Velamakanni, A.; Piner, R. D.; Kang, J.; Park, J.; Ruoff, R. S. *ACS Nano* **2011**, *5*, 1321.

(10) Colson, J. W.; Woll, A. R.; Mukherjee, A.; Levendorf, M. P.; Spitler, E. L.; Shields, V. B.; Spencer, M. G.; Park, J.; Dichtel, W. R. *Science* **2011**, *332*, 228.

(11) Yuk, J. M.; Kim, K.; Alemán, B. n.; Regan, W.; Ryu, J. H.; Park, J.; Ercius, P.; Lee, H. M.; Alivisatos, A. P.; Crommie, M. F.; Lee, J. Y.; Zettl, A. *Nano Lett.* **2011**, *11*, 3290.

(12) (a) Sun, Z.; Kohama, S.-i.; Zhang, Z.; Lomeda, J.; Tour, J. *Nano Res.* **2010**, *3*, 117. (b) Lim, H.; Lee, J. S.; Shin, H.-J.; Shin, H. S.; Choi, H. C. *Langmuir* **2010**, *26*, 12278.

(13) Dreyer, D. R.; Park, S.; Bielawski, C. W.; Ruoff, R. S. *Chem. Soc. Rev.* **2010**, *39*, 228.

(14) Zhang, T.; Cheng, Z.; Wang, Y.; Li, Z.; Wang, C.; Li, Y.; Fang, Y. *Nano Lett.* **2010**, *10*, 4738.

(15) (a) Khokhar, F. S.; van Gastel, R.; Poelsema, B. *Phys. Rev. B* **2010**, *82*, 205409. (b) Wang, Q. H.; Hersam, M. C. *Nat. Chem.* **2009**, *1*, 206.

(16) (a) Cheng, H.-C.; Shiue, R.-J.; Tsai, C.-C.; Wang, W.-H.; Chen, Y.-T. *ACS Nano* **2011**, *5*, 2051. (b) Sun, J. T.; Lu, Y. H.; Chen, W.; Feng, Y. P.; Wee, A. T. S. *Phys. Rev. B* **2010**, *81*, 155403. (c) Coletti, C.; Riedl, C.; Lee, D. S.; Krauss, B.; Patthey, L.; von Klitzing, K.; Smet, J. H.; Starke, U. *Phys. Rev. B* **2010**, *81*, 235401. (d) Yong-Hui, Z.; Zhou, K.-G.; Xie, K.-F.; Zeng, J.; Zhang, H.-L.; Peng, Y. *Nanotechnology* **2010**, *21*, 065201.

(17) Wang, X.; Tabakman, S. M.; Dai, H. *J. Am. Chem. Soc.* **2008**, *130*, 8152.

(18) Xu, Y.; Bai, H.; Lu, G.; Li, C.; Shi, G. *J. Am. Chem. Soc.* **2008**, *130*, 5856.

(19) (a) Padmaja, K.; Wei, L.; Lindsey, J. S.; Bocian, D. F. *J. Org. Chem.* **2005**, *70*, 7972. (b) Yam, C. M.; Cho, J.; Cai, C. *Langmuir* **2004**, *20*, 1228.

(20) (a) Drew, M. E.; Chworos, A.; Oroudjev, E.; Hansma, H.; Yamakoshi, Y. *Langmuir* **2009**, *26*, 7117. (b) Sakata, T.; Maruyama, S.; Ueda, A.; Otsuka, H.; Miyahara, Y. *Langmuir* **2007**, *23*, 2269. (c) Nikitin, K.; Lestini, E.; Lazzari, M.; Altobello, S.; Fitzmaurice, D. *Langmuir* **2007**, *23*, 12147. (d) Kitagawa, T.; Idomoto, Y.; Matsubara, H.; Hobara, D.; Kakiuchi, T.; Okazaki, T.; Komatsu, K. *J. Org. Chem.* **2006**, *71*, 1362. (e) Whitesell, J. K.; Chang, H. K. *Science* **1993**, *261*, 73.

(21) (a) Clark, C. C.; Meyer, G. J.; Wei, Q.; Galoppini, E. *J. Phys. Chem. B* **2006**, *110*, 11044. (b) Galoppini, E. *Coord. Chem. Rev.* **2004**, *248*, 1283. (c) Long, B.; Nikitin, K.; Fitzmaurice, D. *J. Am. Chem. Soc.* **2003**, *125*, 15490. (d) Galoppini, E.; Guo, W.; Qu, P.; Meyer, G. J. *J. Am. Chem. Soc.* **2001**, *123*, 4342.

(22) Otsuki, J.; Shimizu, S.; Fumino, M. *Langmuir* **2006**, *22*, 6056.

(23) Li, W.; Tan, C.; Lowe, M. A.; Abruna, H. D.; Ralph, D. C. *ACS Nano* **2011**, *5*, 2264.

(24) (a) Tasis, D.; Tagmatarchis, N.; Bianco, A.; Prato, M. *Chem. Rev.* **2006**, *106*, 1105. (b) Chen, R. J.; Zhang, Y.; Wang, D.; Dai, H. *J. Am. Chem. Soc.* **2001**, *123*, 3838.

(25) Wopschall, R. H.; Shain, I. *Anal. Chem.* **1967**, *39*, 1514.

(26) Laviron, E. *J. Electroanal. Chem.* **1979**, *101*, 19.

(27) McQueen, E. W.; Goldsmith, J. I. *J. Am. Chem. Soc.* **2009**, *131*, 17554.

(28) (a) Iwasaki, T.; Park, H. J.; Konuma, M.; Lee, D. S.; Smet, J. H.; Starke, U. *Nano Lett.* **2011**, *11*, 79. (b) Yu, Q.; et al. *Nat. Mater.* **2011**, *10*, 443. (c) Li, X.; Magnuson, C. W.; Venugopal, A.; Tromp, R. M.; Hannon, J. B.; Vogel, E. M.; Colombo, L.; Ruoff, R. S. *J. Am. Chem. Soc.* **2011**, *133*, 2816. (d) Ajayan, P. M.; Yakobson, B. I. *Nat. Mater.* **2011**, *10*, 415.